bioRxiv preprint doi: https://doi.org/10.1101/2023.10.19.563072; this version posted October 22, 2023. The copyright holder for this preprint (which was not certified by peer review) is the author/funder, who has granted bioRxiv a license to display the preprint in perpetuity. It is made available under aCC-BY 4.0 International license.

Species-specific dynamics may cause deviations from general biogeographical predictions – evidence from a population genomics study of a New Guinean endemic passerine bird family (Melampittidae).

Ingo A. Müller[1,3,4*], Filip Thörn[1,3,4], Samyuktha Rajan[2], Per Ericson[3], John P. Dumbacher[5], Gibson Maiah[6], Mozes Blom[4], Knud A. Jønsson[3], Martin Irestedt[3]

[1]Department of Zoology, Division of Systematics and Evolution, Stockholm University, Stockholm, Sweden
[2]Department of Zoology, Division of Ethology, Stockholm University, Stockholm, Sweden
[3]Department of Bioinformatics and Genetics, Swedish Museum of Natural History, Stockholm, Sweden
[4]Museum für Naturkunde, Leibniz Institut für Evolutions- und Biodiversitätsforschung, Berlin, Germany
[5]Institute for Biodiversity Science and Sustainability, California Academy of Sciences, San Francisco, CA, USA
[6]New Guinea Binatang Research Centre, Madang, Papua New Guinea

[*] Corresponding author
E-mail: ingo.muller@nrm.se (IM)

bioRxiv preprint doi: https://doi.org/10.1101/2023.10.19.563072; this version posted October 22, 2023. The copyright holder for this preprint (which was not certified by peer review) is the author/funder, who has granted bioRxiv a license to display the preprint in perpetuity. It is made available under aCC-BY 4.0 International license.

Abstract

New Guinea, the largest tropical island, is topographically complex and is dominated by a large central mountain range surrounded by multiple smaller isolated mountain regions along its perimeter. The island is biologically hyper-diverse and harbours an avifauna with many species found only there. The family Melampittidae is endemic to New Guinea and consists of two monotypic genera: *Melampitta lugubris* (Lesser Melampitta) and *Megalampitta gigantea* (Greater Melampitta). Both Melampitta species have scattered and disconnected distributions across New Guinea in the central mountain range and in some of the outlying ranges. While *M. lugubris* is common and found in most montane regions of the island, *M. gigantaea* is elusive and known from only six localities in isolated pockets on New Guinea with very specific habitats of limestone and sinkholes. In this project, we apply museomics to determine the population structure and demographic history of these two species. We re-sequenced the genomes of all seven known *M. gigantaea* samples housed in museum collections as well as 24 *M. lugubris* samples from across its distribution. By comparing population structure between the two species, we investigate to what extent habitat dependence, such as in *M. gigantaea*, may affect population connectivity. Phylogenetic and population genomic analyses, as well as acoustic differentiation, revealed that *M. gigantaea* consists of a single population in contrast to *M. lugubris* that shows much stronger population structure across the island. This work sheds new light on the mechanisms that have shaped the intriguing distribution of the two species within this family and is a prime example of the importance of museum collections for genomic studies of poorly known and rare species.

bioRxiv preprint doi: https://doi.org/10.1101/2023.10.19.563072; this version posted October 22, 2023. The copyright holder for this preprint (which was not certified by peer review) is the author/funder, who has granted bioRxiv a license to display the preprint in perpetuity. It is made available under aCC-BY 4.0 International license.

Introduction

What determines the build-up of biodiversity in space and through time is a long-standing question within biology. The accumulation of phenotypic and genetic differences between populations can only be generated through reproductive isolation that impedes genetic exchange between populations [1,2]. More explicitly, gene flow between diverging populations must be sufficiently limited so that genetic exchange does not exceed the accumulation of differentiation. Barriers underlying reproductive isolation, may differ markedly. They may be postzygotic and arise from genetic incompatibilities, which produce hybrid offspring that have either reduced fitness or are infertile [3–5]. Alternatively, barriers may be prezygotic and decrease the probability of mating events between populations, due to mating preferences, or through geographical (allopatric) or habitat barriers that separate different populations [4–6].

Mountains represent a classic example of geographical barriers both as physical barriers for populations but also because they harbour highly differentiated environments at different elevations. For sedentary lowland populations, mountains may represent unsurpassable barriers, which may over time lead to isolation and differentiation of separate lowland populations. Evidence for such montane barriers restricting gene flow between lowland populations are known from various organismal groups such as amphibians, spiders and coniferous trees [7–9]. Alternatively, extensive lowland valleys can also act as barriers to geneflow between populations adapted to high elevations. Lowland environments may be unsuitable for such mountain-adapted individuals, which over time become isolated on a series of mountaintops or “sky islands” [10,11] as known from some groups of birds, lizards and plants [12–16].

Related to this is the observation that older taxa are often found at higher elevations, while young lineages that are generally widespread, good dispersers and show little

bioRxiv preprint doi: https://doi.org/10.1101/2023.10.19.563072; this version posted October 22, 2023. The copyright holder for this preprint (which was not certified by peer review) is the author/funder, who has granted bioRxiv a license to display the preprint in perpetuity. It is made available under aCC-BY 4.0 International license.

65 differentiation inhabit the lowlands (e.g. 16–19). Such observations (mostly from island
66 systems) have led to the formulation of the concept of taxon cycles, in which taxa pass through
67 phases of expansions and contractions. The concept predicts that over time, taxa move into
68 high elevation habitats either because they are outcompeted by new young taxa in their original
69 (lowland) habitats or because they specialise and adapt to new environments at higher
70 elevations [17,18,20–22].

71 Recent work on the New Guinean avifauna has provided empirical evidence in favour
72 of species originating in the lowlands from where they move into the highlands over time and
73 become relictual specialists [16,22,23], although some colonisation from mountaintop to
74 mountaintop has also been shown to occur [15]. In addition, recent Pleistocene speciation
75 events on New Guinea are mainly the result of changes in habitat distributions due to climate
76 fluctuations, as this has caused species with continuous distributions to become geographically
77 fragmented [24–26]. Pliocene speciation events, on the other hand, are driven mainly by
78 geological processes such as montane uplift, which is known to have caused barriers to gene
79 flow [27–30].

80 The Melampittidae represents an example of an old passerine family with only two
81 deeply diverged species in monotypic genera. Their taxonomic affinities have been difficult to
82 establish, but recent genetic results have placed the family as sister to crows (Corvidae) and
83 shrikes (Laniidae) with an estimated divergence time from these at ca. 17 Mya [31]. One of the
84 species, *Melampitta lugubris* (Lesser Melampitta) is relatively common at high elevations
85 (1150-3500 m asl.), in accordance with the notion that older species tend to occupy higher
86 elevations [21,22,32]. The other species, *Megalampitta gigantea* (Greater Melampitta) is only
87 known from six localities at mid-elevations (650 -1400 m asl.) scattered across New Guinea.
88 Based on few field observations, it is considered to be sedentary and to have limited flight
89 capabilities [33,34]. Within its range, *M. gigantea* is associated with very specific karstic

bioRxiv preprint doi: https://doi.org/10.1101/2023.10.19.563072; this version posted October 22, 2023. The copyright holder for this preprint (which was not certified by peer review) is the author/funder, who has granted bioRxiv a license to display the preprint in perpetuity. It is made available under aCC-BY 4.0 International license.

habitats where it has been observed to spend considerable time nesting in narrow limestone sinkholes in which the birds have to climb in and out [33]. In contrast to *M. lugubris* the distribution of *M. gigantea* does not fit the general pattern that old taxa tend to occupy higher elevation.

In this genomic study we determine the population structure within *M. lugubris* and *M. gigantea* to understand how habitat connectivity across space and through time has shaped differentiation in these two species. Based on the contemporary distributions of the two species we hypothesize that:

1) The 7 individuals of *M. gigantea* represent several distinct evolutionary entities/populations, as the species is a poor disperser and has a fragmented distribution across New Guinea where it is associated with specific karst limestone habitat with sinkholes.
2) Individuals of *M. lugubris* represent a relatively cohesive group, yet with some population structure as deep lowland valleys may prevent gene flow between the various montane populations in the Central Range, the Huon mountains in the northeast and the Arfak mountains in the northwest.

Material & Methods

DNA sampling, sequencing and read processing

In this study, we follow the taxonomy of the IOC World Bird List [35]. We sampled 24 individuals of *Melampitta lugubris* of which 22 were footpads from museum specimens and two were fresh tissue samples. Additionally, we sampled 7 individuals of *Megalampitta gigantaea*, which represent all known samples present in museum collections. One of these

bioRxiv preprint doi: https://doi.org/10.1101/2023.10.19.563072; this version posted October 22, 2023. The copyright holder for this preprint (which was not certified by peer review) is the author/funder, who has granted bioRxiv a license to display the preprint in perpetuity. It is made available under aCC-BY 4.0 International license.

113 samples was a fresh blood sample. The rest were footpads from historical samples (for a
114 detailed list of samples and the museum collections in which they are stored see S1 Table). The
115 work is mainly based on old museum specimens for which the Nagoya Protocol does not apply.
116 The few fresh tissue samples included in the study are from already preserved samples at
117 natural history museums, for which all required permits are available.
118 DNA from fresh blood/tissue samples was extracted using Qiagen's DNeasy Blood and Tissue
119 kits. For DNA extraction and sequencing library preparation of historical samples, we followed
120 a modified version of Meyer and Kircher [36] that proved suitable for avian museum samples
121 [37]. In short, we extract DNA from toepad tissue mainly following the instructions from
122 Qiagen for animal tissue with the addition of Dithiothreitol (DTT) to improve the ligation yield.
123 During library preparation, we treat our samples with USER enzyme to reduce deamination
124 patterns that are typical for fragmented DNA from historical or ancient samples [38]. For a
125 detailed protocol see [37]. Whole genome re-sequencing was performed on Illumina NovaSeq
126 6000 machines on S4 flow cells going through 200 cycles with a read length of 2 x 100 bp at
127 the National Genomics Infrastructure (NGI) in Stockholm. Up to 24 samples with four libraries
128 each were multiplexed on a single flow cell lane.
129 Sequenced reads were then polished using the reproducible *Nextflow* workflow *nf-polish*
130 *(*https://github.com/MozesBlom/nf-polish) [39,40] (see S2 Table for specific github commits
131 used). This pipeline performs multiple polishing steps, including deduplication, adapter- and
132 quality-based trimming, read merging and the removal of low-complexity reads. Polished reads
133 were then mapped onto a reference genome using *nf-µmap* (https://github.com/IngoMue/nf-
134 umap) applying bwa-mem2 as mapping algorithm and which also allowed us to evaluate the
135 quality control after mapping and investigate damage patterns that are typical for historical
136 DNA [41,42]. We used the hooded crow (*Corvus cornix*, Refseq GCF_000738735.5, [43]) as

bioRxiv preprint doi: https://doi.org/10.1101/2023.10.19.563072; this version posted October 22, 2023. The copyright holder for this preprint (which was not certified by peer review) is the author/funder, who has granted bioRxiv a license to display the preprint in perpetuity. It is made available under aCC-BY 4.0 International license.

our reference genome as it represents a reasonable closely related species with a high-quality chromosome level assembly [31].

Phylogenetic analyses on mitochondrial and nuclear DNA

To assemble the full mitogenome from our polished reads we used nf_mito-mania with default settings (https://github.com/FilipThorn/nf_mito-mania) [44]. Variant calling implemented in this pipeline filters sites with a depth-of-coverage below 20 or above three times the average depth-of-coverage across the whole mitogenome of each individual. The resulting consensus sequences of every individual were aligned using *MAFFT* (v7.407, [45], see S2 File for specific flags). An occasional artefact of Mitobim where mitochondrial assemblies become longer than they are supposed to be resulted in overhanging sequences in some individuals. These overhangs were then cut out of the alignment after visual inspection using *Geneious Prime 2023.0.4* so that the final alignment consisted only of overlapping reads (total length 17 112 bp including gaps), which were then used as input for *RAxML-NG* (v1.1.0, [46] using the GTR+G substitution model, 100 bootstrapping replicates and ten randomized parsimony starting trees to generate a mitochondrial phylogenetic tree. Mitochondrial assemblies were also forced into diploid variant calls to check for contamination in our samples. As mitochondria are haploid, heterozygote sites are not expected and could therefore be indicative of cross-contamination.

For the nuclear phylogenetic tree, we used the previously mapped .bam files excluding individuals with very low mean depth-of-coverage (n = 3, DoC < 4 *x*) to call variants for each individual using *freebayes* (v1.3.1-dirty, [47]). Polymorphic sites were filtered based on their quality score (> 20), allelic balance (≥ 0.2), and minimum and maximum depth-of-coverage (3 *x* / 100 *x*). We also decomposed multiple nucleotide polymorphisms (MNPs) into single nucleotide polymorphisms (SNPs) and masked heterozygous positions and indels. These filtered .vcf files were then used as input files for the reproducible *Nextflow* workflow *nf-phylo* with default settings (https://github.com/MozesBlom/nf-phylo) [48] to generate both

bioRxiv preprint doi: https://doi.org/10.1101/2023.10.19.563072; this version posted October 22, 2023. The copyright holder for this preprint (which was not certified by peer review) is the author/funder, who has granted bioRxiv a license to display the preprint in perpetuity. It is made available under aCC-BY 4.0 International license.

concatenated (*IQtree2*) and summary coalescent (*ASTRAL3*) species trees based on 'gene' trees of different window-sizes (2000, 5000, 10000, 20000 base pairs).

Population structure and differentiation

To quantify population substructure and to estimate levels of differentiation between samples, we used a genotype likelihood approach as implemented in ANGSD (v0.938) as this is better suited for low coverage data [49]. Specific commands and the filters used are explained in the S2 File. The filters we used for admixture and principal component analyses (PCAs) were slightly different from those used to calculate nucleotide diversity, heterozygosity and Tajima's D. As we did not have an ancestral genome available, we used the reference genome as ancestral sequence and folded the site frequency spectra (SFS). PCAs were performed through *PCAngsd* [50] and plotted with custom R scripts through RStudio (v 2023.03.0 build 386, R version 4.1.1, [51,52]). Admixture analyses to determine population structure was run through *NgsAdmix* [53] running up to K = 10 with ten replicates for each K and visualised with custom R scripts. Individual heterozygosity was estimated by generating a site frequency spectrum for each individual and dividing the number of sites with one derived allele divided by the total number of sites as performed by e.g. Hansen et al. [54]. Using SFS for each species, nucleotide diversity and Tajima's D were both estimated for each chromosome as well as in 20 kb windows sliding in steps of 10 kb using the *thetaStat* command. We divided the pairwise theta estimator (*tP*) by the total number of Sites (*nSites*) of each chromosome/window to calculate nucleotide diversity. Statistical significance of differences in heterozygosity and nucleotide diversity between the two species was checked using Welch's t-test after verifying normal distributions and inequal variances within the data.

bioRxiv preprint doi: https://doi.org/10.1101/2023.10.19.563072; this version posted October 22, 2023. The copyright holder for this preprint (which was not certified by peer review) is the author/funder, who has granted bioRxiv a license to display the preprint in perpetuity. It is made available under aCC-BY 4.0 International license.

Estimation of effective population sizes through time and divergence times

To estimate effective population sizes through time, we used pairwise sequentially Markovian coalescent (PSMC) [55] (for details on the method see S1 file). As an estimate of the neutral genomic mutation rate per generation we used $4.6*10^{-9}$ as obtained in a study of the collared flycatcher *Ficedula albicollis* [56]. We set the estimated generation time for *M. lugubris* to 3.90 years and for *M. gigantea* to 4.58 years [57]. The parameters for the PSMC analysis were set to " -N30 -t5 -r5 -p 4 + 30*2 + 4 + 6 + 10" following Nadachowska-Brzyska et al. [58]. The authors observed no significant change in curve shape when modifying the atomic vectors parameter (-p) and applied the same settings to several different avian species. We only ran PSMCs for the two samples of *M. gigantea* with the highest depth-of-coverage and for each of the five identified clusters within *M. lugubris* (West, Central, East, Huon, Southeast). False negative rates (FNRs) were adjusted based on depth-of-coverage. If depth-of-coverage was higher than 15 X, FNR was kept at 0. However, if individual A had a depth-of-coverage higher than 15 X and individual B had a depth-of-coverage below 15 X, then individual B would have an FNR of $0.1 + 0.1 * x$, where x is the depth-of-coverage of individual A divided by depth-of-coverage of individual B. If both individuals had a depth-of-coverage < 15 X, we used 0.1 for both individuals.

To estimate divergence times between the two species, but also between the different subpopulations of *M. lugubris*, we first ran F_1-hybrid PSMC (hPSMC, [59]) using the same parameters as for the previous PSMC analyses and implementing 100 bootstraps replicates. Additionally, we estimated mitochondrial divergences within and between the two species and subpopulations of *M. lugubris* using the previously generated mitochondrial alignments. We applied the simple "2% rule" which assumes that in birds, the average divergence between two

bioRxiv preprint doi: https://doi.org/10.1101/2023.10.19.563072; this version posted October 22, 2023. The copyright holder for this preprint (which was not certified by peer review) is the author/funder, who has granted bioRxiv a license to display the preprint in perpetuity. It is made available under aCC-BY 4.0 International license.

208 species is 2% per million years [60]. We compared these divergence time estimates with those
209 obtained from the hPSMC analyses.

210 Acoustic recordings and analysis

211 Acoustic recordings of 10 *M. gigantea* individuals and 28 *M. lugubris* individuals were
212 obtained from an online repository of avian vocalizations (https://xeno-canto.org/), which
213 covered different locations across New Guinea. We included all types of vocalisations- songs,
214 calls and vocalisations of an unknown type in the analysis, unless the function of the
215 vocalisation was specified by the recordist (eg: alarm). This is due to the high uncertainty in
216 estimating the type of vocalisation in *M. lugubris,* and visual comparison between vocalisations
217 classified as 'songs' versus 'calls' between individuals recorded in the same location, often
218 showed that they were the same. The vocalisations of each individual (median = 9
219 vocalisations/individual) were measured by a single author (SR) using the Luscinia sound
220 analysis program (version 2.17.11.22.01, [61]).
221 Each vocalisation was visualised using a Gaussian windowing function with the following
222 spectrogram settings: 13 kHz maximum frequency, 5 ms frame length, 221 spectrograph points,
223 80% spectrograph overlap, 80 dB dynamic range, 30% dereverberation, and 50 ms of
224 dereverberation range. Elements were measured as continuous sound traces and then grouped
225 into syllables within each vocalisation (each vocalisation contained only one syllable).
226 The vocalisations were then compared using the dynamic time warping algorithm (DTW) in
227 Luscinia, following the same settings used in Wheatcroft et al. [62] that has provided reliable
228 grouping outputs for other songbird species. The final output of the DTW analysis was an
229 acoustic dissimilarity matrix, from which we extracted 10 principal components using
230 nonmetric multidimensional scaling.

bioRxiv preprint doi: https://doi.org/10.1101/2023.10.19.563072; this version posted October 22, 2023. The copyright holder for this preprint (which was not certified by peer review) is the author/funder, who has granted bioRxiv a license to display the preprint in perpetuity. It is made available under aCC-BY 4.0 International license.

Results

Our evaluation of mapped reads against the *Corvus cornix* genome showed a median depth-of-coverage (DoC) of ~ 9.252 *x* (min: 0.026 *x*, max: 30.935 *x*, SD: 7.444) and a median percentage of mapped reads at 89.5 % (min 0.2 %:, max: 95.8 %, SD: 23.693). Detailed values for each individual are listed in S1 Table.

During contamination control using mitochondrial assemblies, we observed an increased amount of heterozygote sites across the libraries in 6 individuals (S3 Table). Upon manual inspection using *Geneious Prime* we found that these heterozygote positions mostly appear in blocks and often within the same regions. This suggests that they were in fact nuclear mitochondrial sequences (NUMTs) that were wrongly mapped onto the mitochondrial genome instead of being a result of contamination. We also observed that non-reference alleles often appeared at a lower frequency (98.093 % of heterozygote sites had a reference allele frequency > 0.5, median reference allele frequency across all heterozygote sites at 0.874) and therefore disappeared during consensus calling, as the more frequent allele gets chosen during this step. Nonetheless, we manually excluded two regions from all samples with blocks (in total 5 700 bp out of the entire alignment's 17 112 bp) of heterozygote sites shared across the majority of individuals. The remaining 11 412 bp were used to generate the mitochondrial phylogenies.

Phylogenetic analyses on mitochondrial and nuclear DNA

We found high congruence between phylogenies built from mitochondrial and nuclear genomes (Fig. 1 A and S1 Fig.). Different window sizes and summary coalescent vs concatenated nuclear phylogenies also had little effect on the topology. We recovered three main clusters within *M. lugubris* that correspond to the geographic location of the samples on an east to west axis (Fig. 1). These clusters also align with previously described subspecies of *M. lugubris* [34]. The first cluster within *M. lugubris* consists of individuals inhabiting the

bioRxiv preprint doi: https://doi.org/10.1101/2023.10.19.563072; this version posted October 22, 2023. The copyright holder for this preprint (which was not certified by peer review) is the author/funder, who has granted bioRxiv a license to display the preprint in perpetuity. It is made available under aCC-BY 4.0 International license.

Birds-Head of north-western New Guinea as well as an individual in the westernmost part of the Central Range. The next cluster inhabits the western and central parts of the Central Range of New Guinea, and the third cluster inhabits the eastern and south-eastern section of the Central Range as well as the isolated outlying Huon mountains. *M. gigantaea*, on the other hand, shows little differentiation between individuals compared to *M. lugubris*. Relationships within *M. gigantaea* are also in accordance with the geographical locality of the samples.

Fig. 1. A Distribution map and sampling sites of Megalampitta gigantaea (orange distribution) and M. lugubris (blue distribution), subclusters of M. lugubris are also coloured differently. Shapefiles for administrative boundaries were obtained from geoBoundaries *[63]*, the map was created using QGIS *[64]*. **B Nuclear phylogeny of Melampittidae** (based on concatenated 5 kbp window alignments) highlighting the subdivisions within M. lugubris (West, Central, East, Huon, Southeast), support values next to the main branches show Bootstraps/site concordance factors (sCF)/window concordance factors (wCF).

Population structure and differentiation

We recover the same pattern of lower levels of differentiation in *M. gigantaea* compared to *M. lugubris* in the PCAs (Fig. 2 A), Heterozygosity (Fig. 2 B), nucleotide diversity (π, S4 Table, S2 Fig.) and admixture (Fig. 2 C). For *M. lugubris* Tajima's D was consistently negative with a mean value of -0.902 (SD: 0.126, median: -0.897, S5 Table, S3 Fig.) which is indicative of either population expansion or a selective sweep. In *M. gigantaea* values for Tajima's D were slightly above zero in the range of 0 – 0.2 (mean 0.103, SD: 0.040, median: 0.112, S5 Table, S3 Fig.). Positive values of Tajima's D could indicate a reduction in population size or balancing selection acting, however as the values are so close to zero the population may just evolve neutrally. In the PCA (Fig. 2 A), PC1 separates the two species, afterwards *M. gigantaea* remains closely clustered up to PC4, while subgroups corresponding to geographic localities make up clusters within *M. lugubris* (S4 Fig.). The two distinct clusters of *M. lugubris* on PC2 (Fig. 2 A) separate eastern New Guinean populations and northwestern New Guinean populations as also observed in the phylogenetic tree (Fig. 1 B). Both heterozygosity and nucleotide diversity were significantly lower in *M. gigantaea* than in *M. lugubris*. Although we

bioRxiv preprint doi: https://doi.org/10.1101/2023.10.19.563072; this version posted October 22, 2023. The copyright holder for this preprint (which was not certified by peer review) is the author/funder, who has granted bioRxiv a license to display the preprint in perpetuity. It is made available under aCC-BY 4.0 International license.

observed a clear trend of increasing heterozygosity with higher depth-of-coverage, the slopes for each population were similar and consistently higher in all but one population of *M. lugubris* (S5 Fig.). Admixture analysis revealed no substructure within *M. gigantaea* from K=2 to K = 7. For *M. lugubris* the observed clusters between K = 2-6 align with the clusters observed in the phylogenetic trees and in the PCAs. Further subdivisions within the main clusters of *M. lugubris* at higher values of K are also corresponding to the populations' geographical location.

Fig. 2. Genetic differentiation in Melampittidae. A) PCA showing the first two principal components for both species. Subclusters of Melampitta lugubris are also coloured differently. **B)** Admixture analysis from K = 1 to K = 6 **C)** Heterozygosity for all individuals between both species.

Estimation of effective population size in time and divergence times

PSMC curves (Fig. 3) for samples from the same populations had similar shapes, but not entirely overlapping as depth-of-coverage varied between samples. Within *M. lugubris* the shape of the curves varied, but most of this variation could be ascribed to population specific events. In *M. gigantaea*, we observe an effective population size peak at around 200 Kya followed by a steady decline in effective population size up until around 40 Kya.

The divergence time obtained from hPSMCs curves for the split between *M. gigantaea* and *M. lugubris* was estimated to about 10 mya (S6 Fig.). Splits between subgroups within *M. lugubris* were estimated more recently with the split between Western+Vogelkop and Eastern populations at around 4-5 mya (S7 Fig.) and between Western and Vogelkop populations at about 3-4 mya (S8 Fig.). The next divisions within Eastern *M. lugubris* populations (East, Huon and Southeast) happened at similar times around 1 mya (S8 and S9 Figs.).

Fig. 3. PSMC plots for two representative individuals of **A)** Megalampitta gigantaea **B)** Melampitta lugubris western population **C)** M. lugubris central population **D)** M. lugubris eastern population and Huon, colours in **D)** represent the Huon (blue) and (South)Eastern (purple) subclusters.

bioRxiv preprint doi: https://doi.org/10.1101/2023.10.19.563072; this version posted October 22, 2023. The copyright holder for this preprint (which was not certified by peer review) is the author/funder, who has granted bioRxiv a license to display the preprint in perpetuity. It is made available under aCC-BY 4.0 International license.

Mitochondrial divergences were, as expected, highest for comparisons between the *M. gigantaea* and *M. lugubris* and its subpopulations at a range of 9.8 – 13.3 %. Divergence within *M. gigantaea* was also lower (mean 0.912 %) than within *M. lugubris* (mean 4.979 %) or even in some of its subpopulations. For an extensive table with all comparisons of mitochondrial divergence see S11 and S12 Figs.. Divergence times obtained through the 2% rule were 4.9 – 6.6 mya for the split between *M. gigantaea* and *M. lugubris*, 3.7 – 5.6 mya for splits between Western+Vogelkop populations from Eastern populations of *M. lugubris* and Western populations from Vogelkop populations at 3.6 - 3.8 mya. Subdivisions within the Eastern populations were estimated at 0.2 – 2.7 mya.

Acoustic recordings and analysis

The first ten principal components collectively explained 97% of the variation in vocalisations across the two *Melampitta* species. PC1, which explained 44.5% of the variation in all vocalisations, was more varied for *M. lugubris* (standard deviation (SD) = 0.086) compared to *M. gigantaea* (SD = 0.036). The same was true for PC2, where the standard deviation was once again higher for *M. lugubris* (SD = 0.11) compared to *M. gigantaea* (SD = 0.017). These results show that *M. lugubris* has greater acoustic diversity than *M. gigantaea* (Fig. 4).

Fig. 4. Acoustic variation across species: Principal component space (PC1-2) of vocalisations from M. gigantaea and M. lugubris. PC1 and PC2 scores are averaged within individuals and triangles represent species centroids. Ellipses contain 95% of vocalisations of each species. The Significant outlier within M. lugubris may represent an odd vocalisation that is not directly comparable with the other vocalisations included here. Note that vocalisations for M. gigantaea were only available from three localities (the Fakfak mountains in the Bird's Neck, a locality in the southern Bird's Neck and Tabubil in the central highlands) and vocalisations for M. lugubris were only available from two of the three distinct clades (samples were available from the western and central but no vocalisation data was available from the eastern and Huon populations).

bioRxiv preprint doi: https://doi.org/10.1101/2023.10.19.563072; this version posted October 22, 2023. The copyright holder for this preprint (which was not certified by peer review) is the author/funder, who has granted bioRxiv a license to display the preprint in perpetuity. It is made available under aCC-BY 4.0 International license.

Discussion

The formation of the avifauna on New Guinea largely follows the predictions of taxon cycles [15,16] whereby new species form in or colonise through the lowlands and over time move upwards and become relictual at high elevations. The family Melampittidae is a species-poor old endemic lineage of New Guinea [31]. The family includes two extant species of which one (*Melampitta lugubris*) follows the general taxon-cycle expectation in that it is an old lineage that inhabits montane forests of New Guinea. The other species, *Megalampitta gigantea,* however, has a distribution associated with specific karst habitats at lower elevations and in foothills [34].

Our divergence time estimates suggest that *M. gigantea* and *M. lugubris* diverged from each other in the Miocene (at approximately 10 Mya based on hPSMC results), which is slightly younger than the divergence time estimated by Jønsson et al.[65] and slightly older than the divergence time estimated by McCullough et al. [66]. The three main populations of *M. lugubris* (Fig. 1 B) diverged from each other in the early Pliocene (at approximately 4-5 Mya based on hPSMC curves). A Pliocene divergence of *M. lugubris* populations coincides with major uplift of various mountain regions on New Guinea [67–69], which may have shaped the present population structure of *M. lugubris*. The distributional pattern of populations of *M. lugubris*, with one distinct Vogelkop population and a division of an eastern and a western population along the central mountain range, is also a pattern similar to that found in other New Guinean mountain birds with Pliocene divergences [30,70,71].

The PSMC curves of the three main populations of *M. lugubris* differ (Fig. 3), yet with a general trend of increasing population sizes towards the present. The exception to this is the population of the Huon mountains, which shows a continuous decrease in population size since approximately 100 Kya. Our interpretation is that eastern and south-eastern populations of the

bioRxiv preprint doi: https://doi.org/10.1101/2023.10.19.563072; this version posted October 22, 2023. The copyright holder for this preprint (which was not certified by peer review) is the author/funder, who has granted bioRxiv a license to display the preprint in perpetuity. It is made available under aCC-BY 4.0 International license.

359 Central Range have maintained continuous gene flow, while the connectivity with the Huon
360 population was broken or at least severely reduced as this population became isolated in the
361 outlying Huon Mountain range.
362
363 Given a presumed poor dispersal capacity [33] and a patchy distribution at mid-elevations, we
364 initially hypothesised that *M. gigantea* would exhibit a clear population structure. However,
365 contrary to expectations, all our samples of *M. gigantea*, from localities scattered across New
366 Guinea, cluster tightly together genetically (Fig. 1 and Fig**. 2**). Analysis of vocalisations also
367 shows a similar pattern, as *M. gigantea* compared to *M. lugubris* exhibits less vocal
368 differentiation (Fig. 4). This is fascinating and difficult to explain. Below, we discuss three
369 scenarios that may provide possible explanations for these patterns. First, it is possible that
370 continuous migration (or high rates of juvenile dispersal) of *M. gigantea* individuals maintains
371 contact and gene flow between populations. However, an exclusively ground-dwelling lifestyle
372 and the lack of long-distance flight capabilities, suggested by its morphology and field
373 observations contradict this scenario [33,34]. Second, it is possible that their presently known
374 fragmented distribution does not properly reflect their actual distribution, which may be more
375 extensive [34,72]. Karst regions are generally species-poor in comparison to the species-rich
376 tropical forests of New Guinea and such localised karstic areas dispersed throughout New
377 Guinea may therefore have commanded less attention by ornithological surveys. Finally, it is
378 possible that *M. gigantea* once had a wider more continuous distribution and that a recent
379 decline has left scattered populations in small pockets of Karst habitat. The PSMC analyses
380 support this scenario by showing that the population size of *M. gigantea* has dropped
381 dramatically within the last 200 Ky (Fig. 3). The fact that *M. gigantea* is highly adapted to a
382 very specific habitat type (nesting in deep holes in karst limestone that they have to climb out
383 of [33] is, however, difficult to reconcile with this scenario. However, one may speculate that

bioRxiv preprint doi: https://doi.org/10.1101/2023.10.19.563072; this version posted October 22, 2023. The copyright holder for this preprint (which was not certified by peer review) is the author/funder, who has granted bioRxiv a license to display the preprint in perpetuity. It is made available under aCC-BY 4.0 International license.

384 *M. gigantea* in the past had broader habitat preferences not only restricted to the present karst
385 limestone habitats. Perhaps during the last 200 Ky, increased competition from other species
386 forced *M. gigantea* to retract to a particular low-diversity habitat type, leaving behind the
387 scattered distribution that we see today. Overall, we find it most plausible, that *M. gigantea*
388 had a larger and more continuous distribution in the past, yet we acknowledge that the present
389 distribution may be underestimated. Additional ornithological surveys to suitable habitats may,
390 thus, reveal further *M. gigantea* populations.

391 # Conclusions

392 In this study, the rather surprising population structure of the two species of an old New
393 Guinean avian family have been elucidated by genomic data largely obtained from historical
394 museum collections. While the population structure of *Melampitta lugubris* is similar to those
395 found in other mountain birds of New Guinea with similar age, the population structure of
396 *Megalampitta gigantea* is intriguing. The study is an example of how intrinsic properties, such
397 as those exhibited by *M. gigantea*, may cause their population dynamics to deviate from general
398 biogeographical predictions. The study is also an example of how important museum
399 collections are for increasing the knowledge of rare taxa that occur in remote regions. The
400 levels of divergence between the three major populations of *M. lugubris* are well above those
401 at which ornithologists would normally assign species rank. Consequently, we tentatively
402 propose that these three populations should be elevated to species rank, *M. lugubris* (Schlegel,
403 1871) in the Vogelkop region, *Melampitta rostrata* (Ogilvie-Grant, 1913) in the western central
404 range and *Melampitta longicauda* (Mayr & Gilliard, 1952) in the eastern central range.
405

bioRxiv preprint doi: https://doi.org/10.1101/2023.10.19.563072; this version posted October 22, 2023. The copyright holder for this preprint (which was not certified by peer review) is the author/funder, who has granted bioRxiv a license to display the preprint in perpetuity. It is made available under aCC-BY 4.0 International license.

Acknowledgements

Computations were enabled by resources provided by the National Academic Infrastructure for Supercomputing in Sweden (NAISS) and the Swedish National Infrastructure for Computing (SNIC) at UPPMAX partially funded by the Swedish Research Council through grant agreements no. 2022-06725 and no. 2018-05973. Furthermore, the authors acknowledge support from the National Genomics Infrastructure in Stockholm funded by Science for Life Laboratory, the Knut and Alice Wallenberg Foundation and the Swedish Research Council, and SNIC/Uppsala Multidisciplinary Center for Advanced Computational Science for assistance with massively parallel sequencing and access to the UPPMAX computational infrastructure. Lastly, we would like to thank Nikolay Oskolkov for assistance with bioinformatic analyses as part of the drop-in services and the Swedish Bioinformatics Advisory Program of the National Bioinformatics Infrastructure Sweden (NBIS).

References

1. Dobzhansky TG. Genetics of the evolutionary process. Vol. 139. Columbia University Press; 1970.
2. Westram AM, Stankowski S, Surendranadh P, Barton N. What is reproductive isolation? J Evol Biol. 2022;35(9):1143–64.
3. Dobzhansky TG. Studies on Hybrid Sterility. II. Localization of Sterility Factors in Drosophila Pseudoobscura Hybrids. Genetics. 1936 Mar;21(2):113–35.
4. Coyne JA. Genetics and speciation. Nature. 1992 Feb;355(6360):511–5.
5. Turelli M, Barton NH, Coyne JA. Theory and speciation. Trends Ecol Evol. 2001 Jul;16(7):330–43.
6. North HL, Caminade P, Severac D, Belkhir K, Smadja CM. The role of copy-number variation in the reinforcement of sexual isolation between the two European subspecies of the house mouse. Philos Trans R Soc B Biol Sci. 2020 Aug 31;375(1806):20190540.
7. Sánchez-Montes G, Wang J, Ariño AH, Martínez-Solano Í. Mountains as barriers to gene flow in amphibians: Quantifying the differential effect of a major mountain ridge on the genetic structure of four sympatric species with different life history traits. J Biogeogr. 2018;45(2):318–31.
8. Salgado-Roa FC, Pardo-Diaz C, Lasso E, Arias CF, Solferini VN, Salazar C. Gene flow and Andean uplift shape the diversification of Gasteracantha cancriformis (Araneae: Araneidae) in Northern South America. Ecol Evol. 2018;8(14):7131–42.

bioRxiv preprint doi: https://doi.org/10.1101/2023.10.19.563072; this version posted October 22, 2023. The copyright holder for this preprint (which was not certified by peer review) is the author/funder, who has granted bioRxiv a license to display the preprint in perpetuity. It is made available under aCC-BY 4.0 International license.

9. Li YS, Shih KM, Chang CT, Chung JD, Hwang SY. Testing the Effect of Mountain Ranges as a Physical Barrier to Current Gene Flow and Environmentally Dependent Adaptive Divergence in Cunninghamia konishii (Cupressaceae). Front Genet [Internet]. 2019 [cited 2023 Jan 19];10. Available from: https://www.frontiersin.org/articles/10.3389/fgene.2019.00742
10. Heald WF. Sky Island [Internet]. Van Nostrand; 1967. Available from: https://books.google.se/books?id=jPWeuQAACAAJ
11. McCormack JE, Huang H, Knowles LL, Gillespie R, Clague D. Sky islands. Encycl Isl. 2009;4:841–3.
12. Robin VV, Sinha A, Ramakrishnan U. Ancient Geographical Gaps and Paleo-Climate Shape the Phylogeography of an Endemic Bird in the Sky Islands of Southern India. PLOS ONE. 2010 Oct 13;5(10):e13321.
13. Wagner P, Greenbaum E, Malonza P, Branch W. Resolving sky island speciation in populations of East African Adolfus alleni (Sauria, Lacertidae). Salamandra. 2014;50(1):1–17.
14. Zhang D, Hao G, Guo X, Hu Q, Liu J. Genomic insight into "sky island" species diversification in a mountainous biodiversity hotspot. J Syst Evol. 2019 Nov;57(6):633–45.
15. Pujolar JM, Blom MPK, Reeve AH, Kennedy JD, Marki PZ, Korneliussen TS, et al. The formation of avian montane diversity across barriers and along elevational gradients. Nat Commun. 2022 Dec;13(1):268.
16. Kennedy JD, Marki PZ, Reeve AH, Blom MPK, Prawiradilaga DM, Haryoko T, et al. Diversification and community assembly of the world's largest tropical island. Glob Ecol Biogeogr. 2022;31(6):1078–89.
17. Wilson EO. Adaptive Shift and Dispersal in a Tropical Ant Fauna. Evolution. 1959;13(1):122–44.
18. Wilson EO. The Nature of the Taxon Cycle in the Melanesian Ant Fauna. Am Nat. 1961;95(882):169–93.
19. Ricklefs RE, Bermingham E. The concept of the taxon cycle in biogeography. Glob Ecol Biogeogr. 2002;11(5):353–61.
20. MacArthur RH, Wilson EO. The Theory of Island Biogeography. REV-Revised. Princeton University Press; 1967.
21. Ricklefs RE, Cox GW. Taxon Cycles in the West Indian Avifauna. Am Nat. 1972 Mar;106(948):195–219.
22. Pepke ML, Irestedt M, Fjeldså J, Rahbek C, Jønsson KA. Reconciling supertramps, great speciators and relict species with the taxon cycle stages of a large island radiation (Aves: Campephagidae). J Biogeogr. 2019 Jun;46(6):1214–25.
23. Reeve AH, Kennedy JD, Pujolar JM, Petersen B, Blom MPK, Alström P, et al. The formation of the Indo-Pacific montane avifauna [Internet]. bioRxiv; 2022 [cited 2023 Jan 26]. p. 2022.06.15.495085. Available from: https://www.biorxiv.org/content/10.1101/2022.06.15.495085v1
24. Williams DJ, O'Shea M, Daguerre RL, Pook CE, Wüster W, Hayden CJ, et al. Origin of the eastern brownsnake, Pseudonaja textilis (Duméril, Bibron and Duméril) (Serpentes: Elapidae: Hydrophiinae) in New Guinea: evidence of multiple dispersals from Australia, and comments on the status of Pseudonaja textilis pughi Hoser 2003. Zootaxa. 2008 Feb 13;(1703):47–61.
25. Kearns AM, Joseph L, Omland KE, Cook LG. Testing the effect of transient Plio-Pleistocene barriers in monsoonal Australo-Papua: did mangrove habitats maintain genetic connectivity in the Black Butcherbird? Mol Ecol. 2011;20(23):5042–59.

bioRxiv preprint doi: https://doi.org/10.1101/2023.10.19.563072; this version posted October 22, 2023. The copyright holder for this preprint (which was not certified by peer review) is the author/funder, who has granted bioRxiv a license to display the preprint in perpetuity. It is made available under aCC-BY 4.0 International license.

26. Ericson PGP, Irestedt M, She H, Qu Y. Genomic signatures of rapid adaptive divergence in a tropical montane species. Biol Lett. 2021 Jul;17(7):20210089.
27. Rawlings LH, Donnellan SC. Phylogeographic analysis of the green python, Morelia viridis, reveals cryptic diversity. Mol Phylogenet Evol. 2003 Apr 1;27(1):36–44.
28. Dumbacher JP, Fleischer RC. Phylogenetic evidence for colour pattern convergence in toxic pitohuis: Müllerian mimicry in birds? Proc R Soc Lond B Biol Sci. 2001 Oct 7;268(1480):1971–6.
29. Deiner K, Lemmon AR, Mack AL, Fleischer RC, Dumbacher JP. A Passerine Bird's Evolution Corroborates the Geologic History of the Island of New Guinea. PLOS ONE. 2011 May 6;6(5):e19479.
30. Irestedt M, Batalha-Filho H, Roselaar CS, Christidis L, Ericson PGP. Contrasting phylogeographic signatures in two Australo-Papuan bowerbird species complexes (Aves: Ailuroedus). Zool Scr. 2016;45(4):365–79.
31. Oliveros CH, Field DJ, Ksepka DT, Barker FK, Aleixo A, Andersen MJ, et al. Earth history and the passerine superradiation. Proc Natl Acad Sci. 2019 Apr 16;116(16):7916–25.
32. Price TD, Hooper DM, Buchanan CD, Johansson US, Tietze DT, Alström P, et al. Niche filling slows the diversification of Himalayan songbirds. Nature. 2014 May 8;509(7499):222–5.
33. Diamond JM. Melampitta gigantea: Possible Relation between Feather Structure and Underground Roosting Habits. The Condor. 1983 Feb;85(1):89–91.
34. Del Hoyo J, Elliot A, Christie D. Handbook of the Birds of the World, Picathartes to Tits and Chickadees, vol. 12. Lynx Edicions Barc. 2007;
35. Gill F, Donsker DB, Rasmussen PC. IOC World Bird List 13.1 [Internet]. World Bird Names; 2023 [cited 2023 Mar 30]. Available from: https://www.worldbirdnames.org/ioc-lists/crossref
36. Meyer M, Kircher M. Illumina Sequencing Library Preparation for Highly Multiplexed Target Capture and Sequencing. Cold Spring Harb Protoc. 2010 Jun 1;2010(6):pdb.prot5448-pdb.prot5448.
37. Irestedt M, Thörn F, Müller IA, Jønsson KA, Ericson PGP, Blom MPK. A guide to avian museomics: Insights gained from resequencing hundreds of avian study skins. Mol Ecol Resour. 2022;22(7):2672–84.
38. Briggs AW, Stenzel U, Meyer M, Krause J, Kircher M, Pääbo S. Removal of deaminated cytosines and detection of in vivo methylation in ancient DNA. Nucleic Acids Res. 2010 Apr;38(6):e87–e87.
39. Di Tommaso P, Chatzou M, Floden EW, Barja PP, Palumbo E, Notredame C. Nextflow enables reproducible computational workflows. Nat Biotechnol. 2017 Apr;35(4):316–9.
40. Blom MPK. nf-polish [Internet]. 2021. Available from: https://github.com/MozesBlom/nf-polish
41. Müller IA. nf-µmap [Internet]. 2022. Available from: https://github.com/IngoMue/nf-umap
42. Vasimuddin Md, Misra S, Li H, Aluru S. Efficient Architecture-Aware Acceleration of BWA-MEM for Multicore Systems. In: 2019 IEEE International Parallel and Distributed Processing Symposium (IPDPS). 2019. p. 314–24.
43. Poelstra JW, Vijay N, Bossu CM, Lantz H, Ryll B, Müller I, et al. The genomic landscape underlying phenotypic integrity in the face of gene flow in crows. Science. 2014 Jun 20;344(6190):1410–4.
44. Thörn F. nf_mito-mania [Internet]. 2022 [cited 2023 Mar 30]. Available from: https://github.com/FilipThorn/nf_mito-mania

bioRxiv preprint doi: https://doi.org/10.1101/2023.10.19.563072; this version posted October 22, 2023. The copyright holder for this preprint (which was not certified by peer review) is the author/funder, who has granted bioRxiv a license to display the preprint in perpetuity. It is made available under aCC-BY 4.0 International license.

45. Katoh K, Standley DM. MAFFT multiple sequence alignment software version 7: improvements in performance and usability. Mol Biol Evol. 2013;30(4):772–80.
46. Kozlov AM, Darriba D, Flouri T, Morel B, Stamatakis A. RAxML-NG: a fast, scalable and user-friendly tool for maximum likelihood phylogenetic inference. Bioinformatics. 2019 Nov 1;35(21):4453–5.
47. Garrison E, Marth G. Haplotype-based variant detection from short-read sequencing [Internet]. arXiv; 2012 [cited 2023 Sep 8]. Available from: http://arxiv.org/abs/1207.3907
48. Blom MPK. nf-phylo [Internet]. 2023 [cited 2023 Mar 30]. Available from: https://github.com/MozesBlom/nf-phylo
49. Korneliussen TS, Albrechtsen A, Nielsen R. ANGSD: Analysis of Next Generation Sequencing Data. BMC Bioinformatics. 2014 Nov 25;15(1):356.
50. Meisner J, Albrechtsen A. Inferring Population Structure and Admixture Proportions in Low-Depth NGS Data. Genetics. 2018 Oct 1;210(2):719–31.
51. R Core Team. R: A Language and Environment for Statistical Computing [Internet]. Vienna, Austria: R Foundation for Statistical Computing; 2021. Available from: https://www.R-project.org/
52. Posit team. RStudio: Integrated Development Environment for R [Internet]. Boston, MA: Posit Software, PBC; 2023. Available from: http://www.posit.co/
53. Skotte L, Korneliussen TS, Albrechtsen A. Estimating Individual Admixture Proportions from Next Generation Sequencing Data. Genetics. 2013 Sep;
54. Hansen CCR, Hvilsom C, Schmidt NM, Aastrup P, Van Coeverden De Groot PJ, Siegismund HR, et al. The Muskox Lost a Substantial Part of Its Genetic Diversity on Its Long Road to Greenland. Curr Biol. 2018 Dec;28(24):4022-4028.e5.
55. Li H, Durbin R. Inference of human population history from individual whole-genome sequences. Nature. 2011 Jul;475(7357):493–6.
56. Smeds L, Qvarnström A, Ellegren H. Direct estimate of the rate of germline mutation in a bird. Genome Res. 2016 Jan 9;26(9):1211–8.
57. Bird JP, Martin R, Akçakaya HR, Gilroy J, Burfield IJ, Garnett ST, et al. Generation lengths of the world's birds and their implications for extinction risk. Conserv Biol. 2020;34(5):1252–61.
58. Nadachowska-Brzyska K, Li C, Smeds L, Zhang G, Ellegren H. Temporal Dynamics of Avian Populations during Pleistocene Revealed by Whole-Genome Sequences. Curr Biol. 2015 May 18;25(10):1375–80.
59. Cahill JA, Soares AER, Green RE, Shapiro B. Inferring species divergence times using pairwise sequential Markovian coalescent modelling and low-coverage genomic data. Philos Trans R Soc B Biol Sci. 2016 Jul 19;371(1699):20150138.
60. Weir JT, Schluter D. Calibrating the avian molecular clock. Mol Ecol. 2008;17(10):2321–8.
61. Lachlan R. rflachlan/Luscinia [Internet]. 2014. Available from: https://github.com/rflachlan/Luscinia
62. Wheatcroft D, Bliard L, El Harouchi M, López-Idiáquez D, Kärkkäinen T, Kraft FLH, et al. Species-specific song responses emerge as a by-product of tuning to the local dialect. Curr Biol. 2022 Dec 5;32(23):5153-5158.e5.
63. Runfola D, Anderson A, Baier H, Crittenden M, Dowker E, Fuhrig S, et al. geoBoundaries: A global database of political administrative boundaries. PLOS ONE. 2020 Apr 24;15(4):e0231866.
64. QGIS Development Team. QGIS Geographic Information System [Internet]. QGIS Association; 2023. Available from: https://www.qgis.org

bioRxiv preprint doi: https://doi.org/10.1101/2023.10.19.563072; this version posted October 22, 2023. The copyright holder for this preprint (which was not certified by peer review) is the author/funder, who has granted bioRxiv a license to display the preprint in perpetuity. It is made available under aCC-BY 4.0 International license.

584 65. Jønsson KA, Fabre PH, Kennedy JD, Holt BG, Borregaard MK, Rahbek C, et al. A
585 supermatrix phylogeny of corvoid passerine birds (Aves: Corvides). Mol Phylogenet
586 Evol. 2016 Jan 1;94:87–94.
587 66. McCullough JM, Oliveros CH, Benz BW, Zenil-Ferguson R, Cracraft J, Moyle RG, et al.
588 Wallacean and Melanesian Islands Promote Higher Rates of Diversification within the
589 Global Passerine Radiation Corvides. Ho S, editor. Syst Biol. 2022 Oct 12;71(6):1423–
590 39.
591 67. Pigram C, Davies H. Terranes and the accretion history of the Papua New Guinea
592 orogeny. BMR J Aust Geol Geophys. 1987;10:193–212.
593 68. Hall R. Cenozoic geological and plate tectonic evolution of SE Asia and the SW Pacific:
594 computer-based reconstructions, model and animations. J Asian Earth Sci. 2002 Apr
595 1;20(4):353–431.
596 69. Davies HL. The geology of New Guinea-the cordilleran margin of the Australian
597 continent. Episodes J Int Geosci. 2012;35(1):87–102.
598 70. Irestedt M, Batalha-Filho H, Ericson PGP, Christidis L, Schodde R. Phylogeny,
599 biogeography and taxonomic consequences in a bird-of-paradise species complex,
600 Lophorina–Ptiloris (Aves: Paradisaeidae). Zool J Linn Soc. 2017 Oct 1;181(2):439–70.
601 71. Jønsson KA, Reeve AH, Blom MP, Irestedt M, Marki PZ. Unrecognised (species)
602 diversity in New Guinean passerine birds. Emu-Austral Ornithol. 2019;119(3):233–41.
603 72. Diamond J, Bishop KD. What's so special about New Guinea birds? Bull Br Ornithol
604 Club. 2023 Jun;143(2):212–36.
605 73. Kendall MG. Rank correlation methods. 1948;

606

607 Supporting information

608 **S1 Figure. Mitochondrial phylogeny for all individuals**

609 **S2 Figure. Individual nucleotide diversity (π)** is significantly lower in M. gigantaea (orange) than in
610 M. lugubris (blue). The applied statistical test was a Welch's two sample t-test for unequal variances.

611 **S3 Figure. Tajima's D** is consistently negative across all chromosomes in M. lugubris (blue) and
612 slightly positive in M. gigantaea.

613 **S4 Figure. Principal components 1 to 4** describing divisions within subpopulations of M. lugubris
614 (shades of blue/purple) while M. gigantaea (orange) remains a tight cluster.

615 **S5 Figure. Heterozygosity** shows a correlation with increasing depth of coverage (DoC). Slopes are
616 similar between populations/species and M. gigantaea still shows lower Heterozygosity than most M.
617 lugubris populations when comparing individuals with similar DoC. To fit regression lines, we applied
618 Kendall's rank correlation coefficient as it is recommended for smaller sample sizes containing outliers
619 [73].

620 **S6 Figure. PSMC for M. lugubris (blue) and M. gigantaea (orange) and their hybrid PSMC curve**
621 **(red)** to show the divergence time between the two species.

bioRxiv preprint doi: https://doi.org/10.1101/2023.10.19.563072; this version posted October 22, 2023. The copyright holder for this preprint (which was not certified by peer review) is the author/funder, who has granted bioRxiv a license to display the preprint in perpetuity. It is made available under aCC-BY 4.0 International license.

S7 Figure. PSMC for M. lugubris NHMD616019 from Huon (red) and M. lugubris B98503 from Central New Guinea (blue) and their hybrid PSMC curve (purple) to show the divergence time between Eastern populations and Western + Central populations of M. lugubris.

S8 Figure. PSMC for M. lugubris B98503 from Central New Guinea (red) and M. lugubris AMNH293751 from Western New Guinea (blue) and their hybrid PSMC curve (purple) to show the divergence time between Central populations and Western populations of M. lugubris.

S9 Figure. PSMC for M. lugubris NHMD616019 from Huon (red) and M. lugubris AMNH590750 from the Southeast (blue) and their hybrid PSMC curve (purple) to show the divergence time between Huon populations and Southeastern populations of M. lugubris.

S10 Figure. PSMC for M. lugubris NHMD616019 from Huon (red) and M. lugubris B100613 from the East (blue) and their hybrid PSMC curve (purple) to show the divergence time between Huon populations and East populations of M. lugubris.

S11 Figure. Mitochondrial divergence matrix showing the minimum (first value) and maximum (second value) for each comparison of populations and species, M. gigantaea (Meg), M. lugubris (Mel), Eastern populations (EPops) include the subpopulations East, Southeast and Huon.

S12 Figure. Mitochondrial divergence matrix showing the mean divergence for each comparison of populations and species, M. gigantaea (Meg), M. lugubris (Mel), Eastern populations (EPops) include the subpopulations East, Southeast and Huon.

S1 Table. List of samples. Additional information such as sample locality, museum voucher, tissue type, etc. are included. The table also shows mapping statistics (e.g. mapping percentage and depth-of-coverage) for each individual.

S2 Table. Used github commits when running nextflow workflows

S3 Table. Filtered individuals with heterozygous blocks in mtDNA

S4 Table. Individual nucleotide diversity (π). Sheet 1 (Individual) contains statistics calculated for each species using i) all chromosomes and ii) only autosomes (aut.). Sheet 2 (Species-wide) contains estimates averaged across i) all chromosomes and ii) only autosomes (aut.)

S5 Table. Species-wide Tajima's D. Values averaged across i) all chromosomes and ii) only autosomes (aut.)

S1 File. Details on PSMC methodology

S2 File. Codes and parameters settings

A

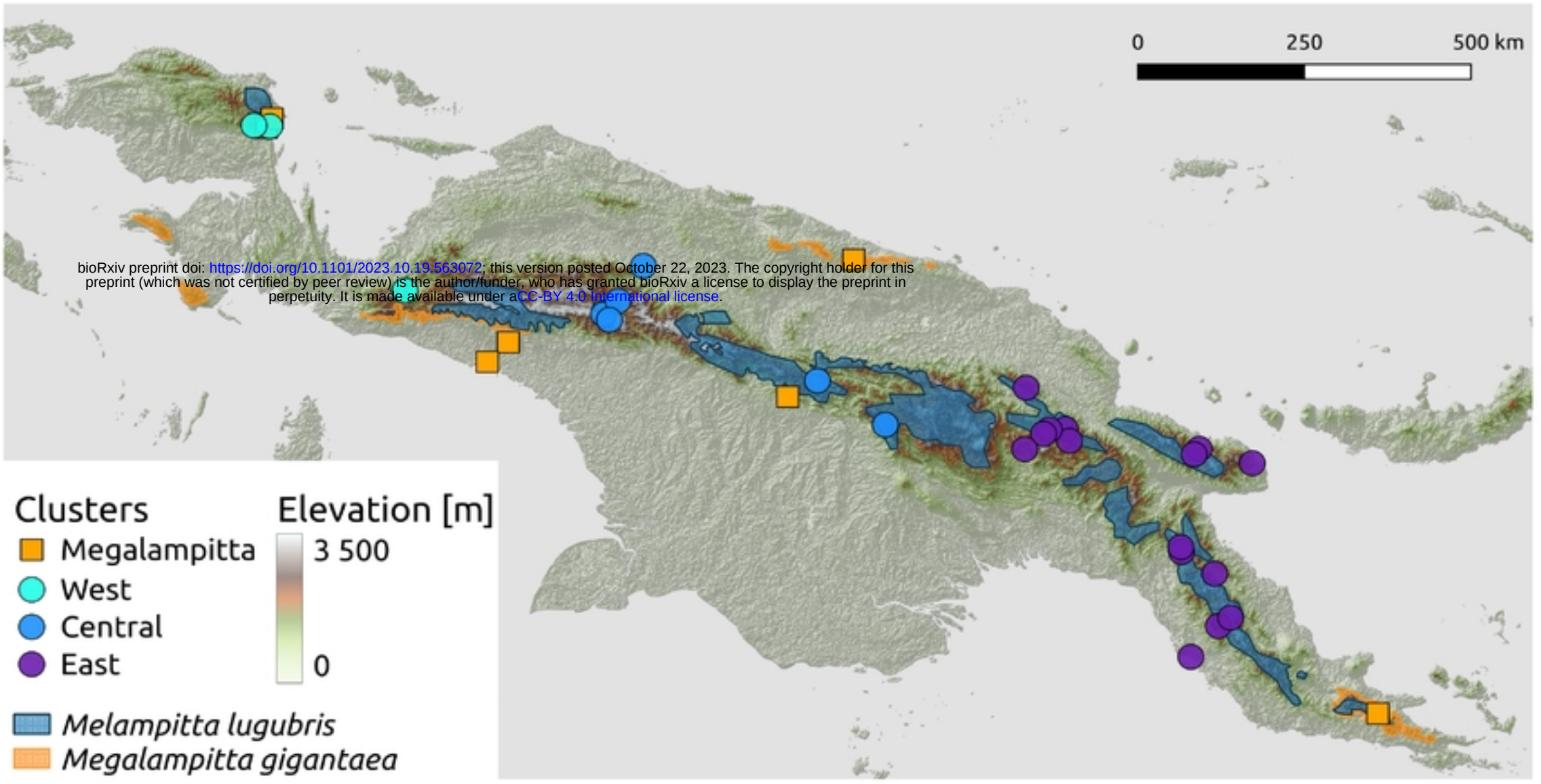

bioRxiv preprint doi: https://doi.org/10.1101/2023.10.19.563072; this version posted October 22, 2023. The copyright holder for this preprint (which was not certified by peer review) is the author/funder, who has granted bioRxiv a license to display the preprint in perpetuity. It is made available under aCC-BY 4.0 International license.

B

Main figure 1

bioRxiv preprint doi: https://doi.org/10.1101/2023.10.19.563072; this version posted October 22, 2023. The copyright holder for this preprint (which was not certified by peer review) is the author/funder, who has granted bioRxiv a license to display the preprint in perpetuity. It is made available under aCC-BY 4.0 International license.

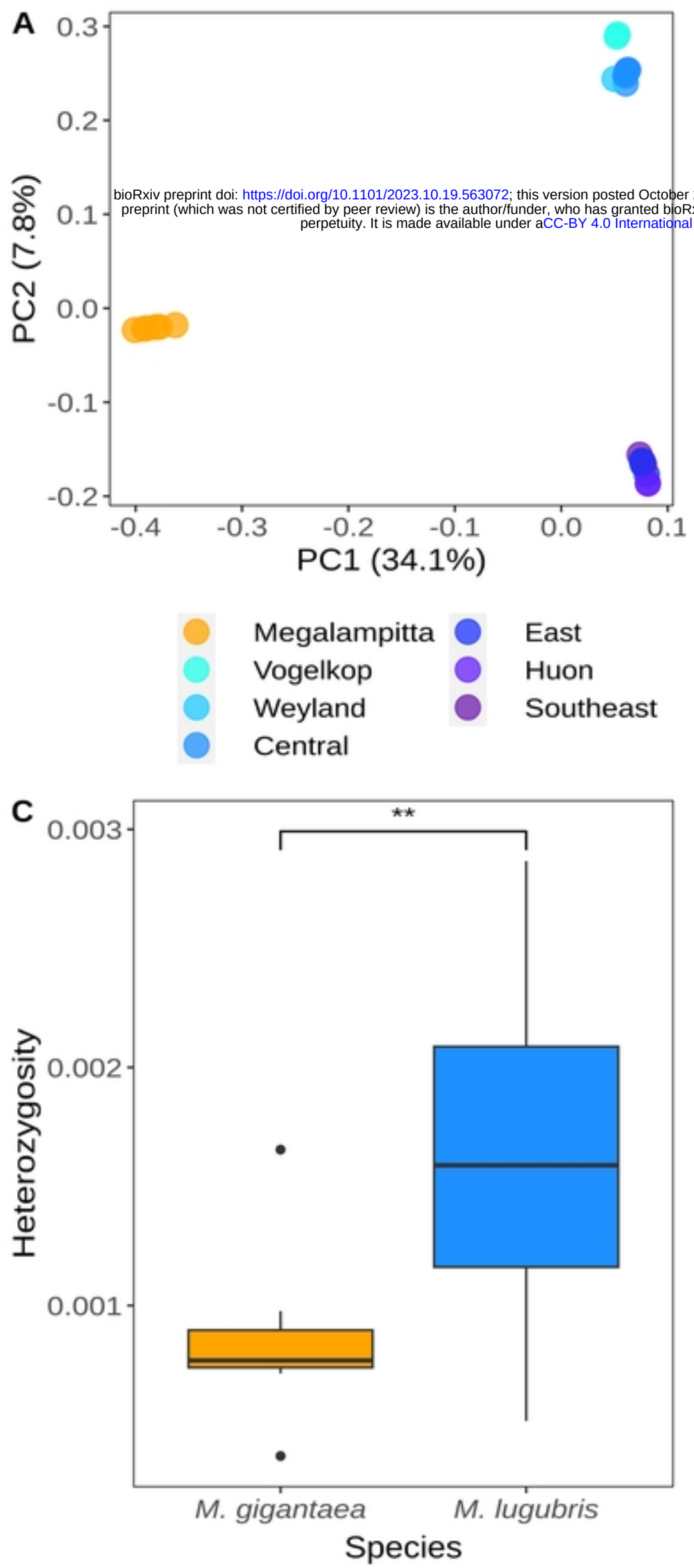

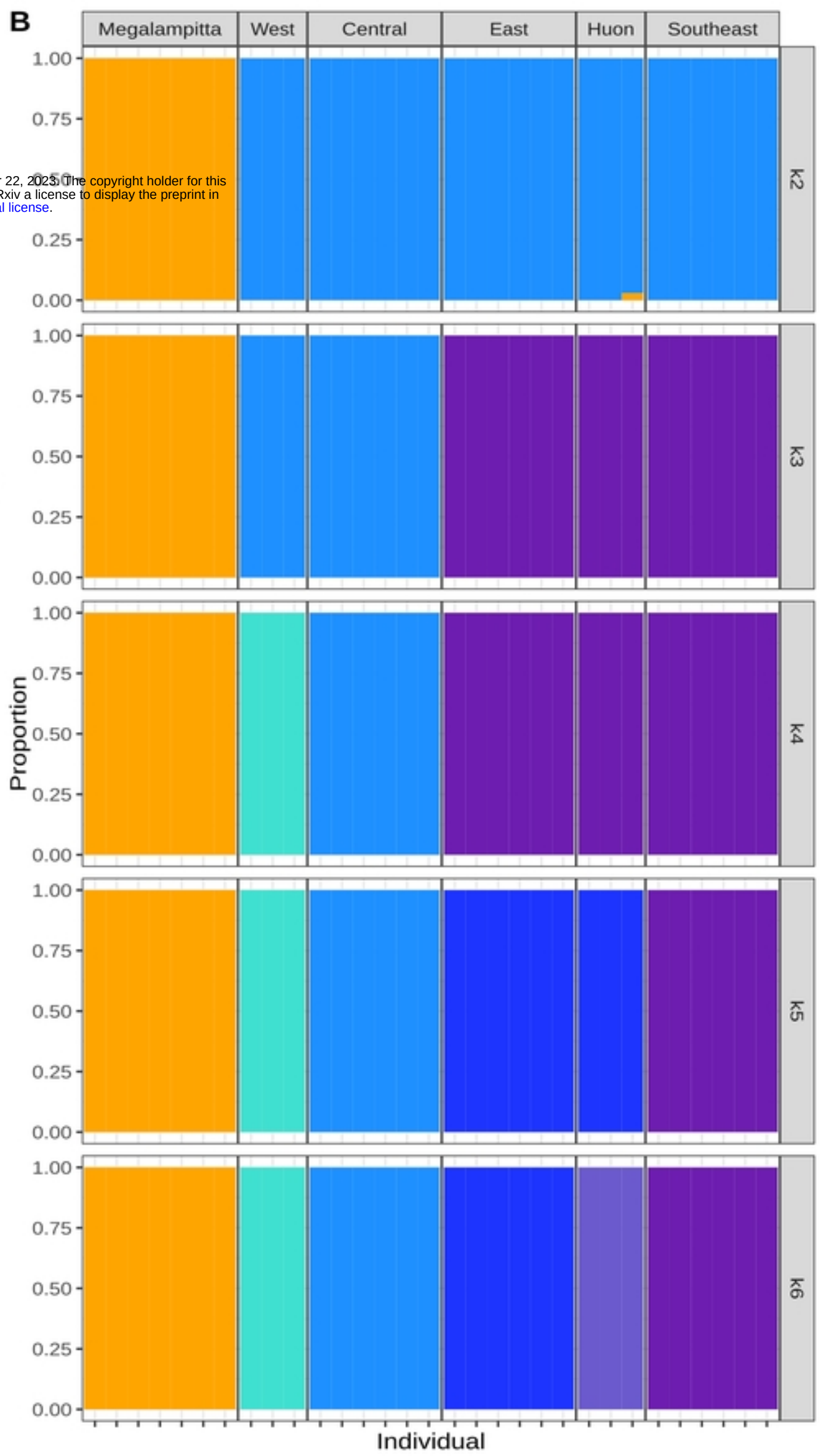

Main figure 2

bioRxiv preprint doi: https://doi.org/10.1101/2023.10.19.563072; this version posted October 22, 2023. The copyright holder for this preprint (which was not certified by peer review) is the author/funder, who has granted bioRxiv a license to display the preprint in perpetuity. It is made available under aCC-BY 4.0 International license.

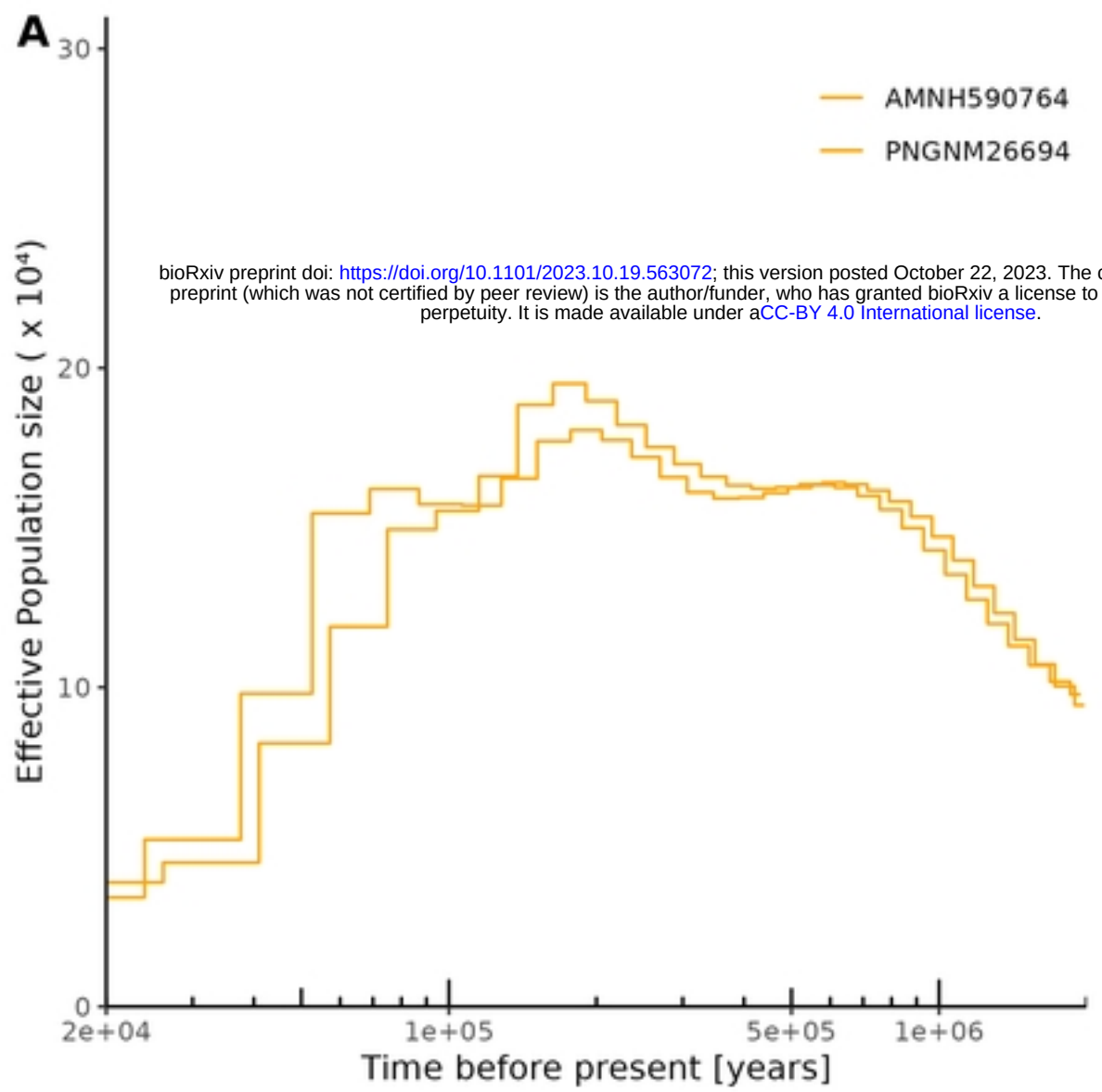

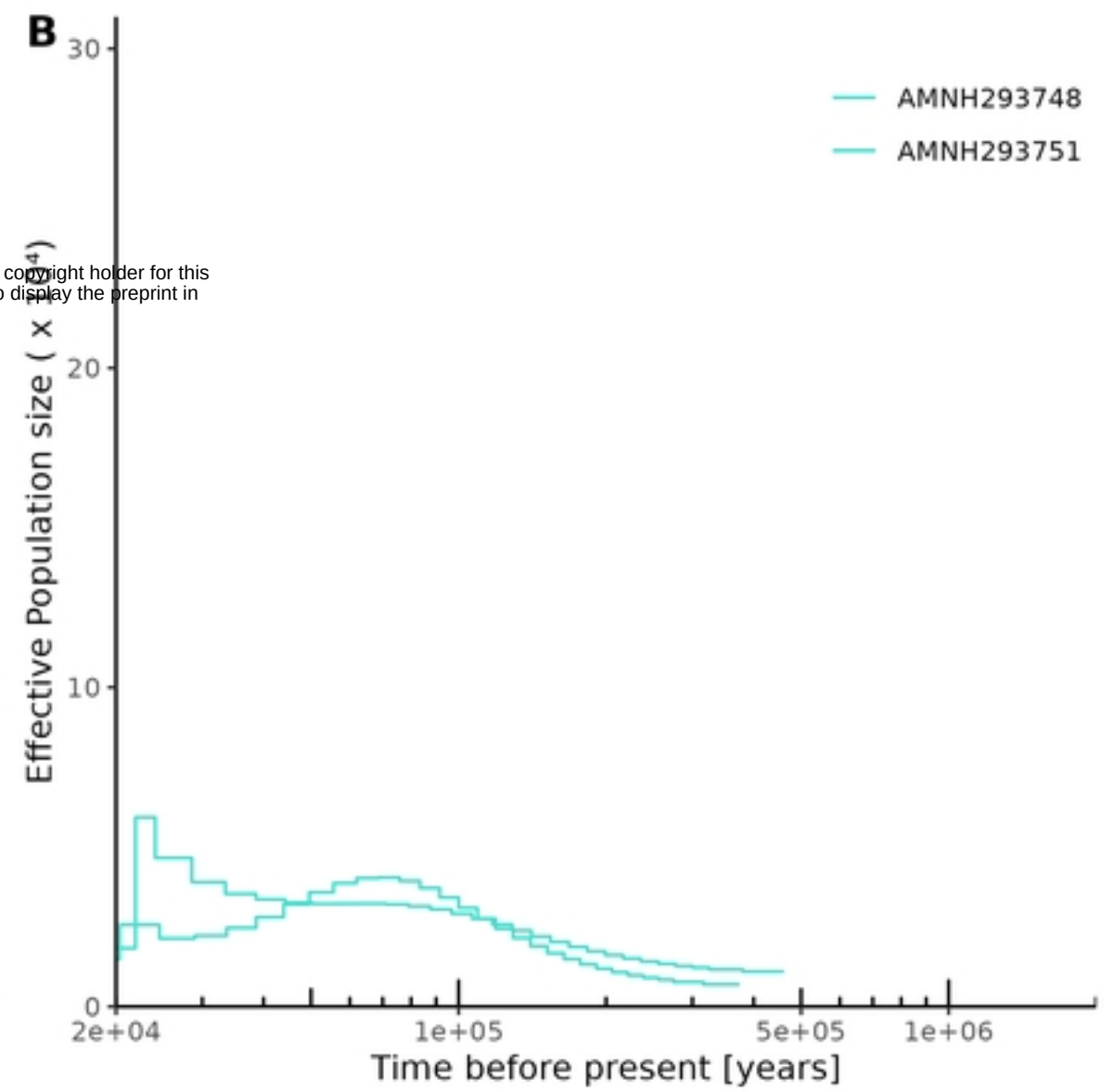

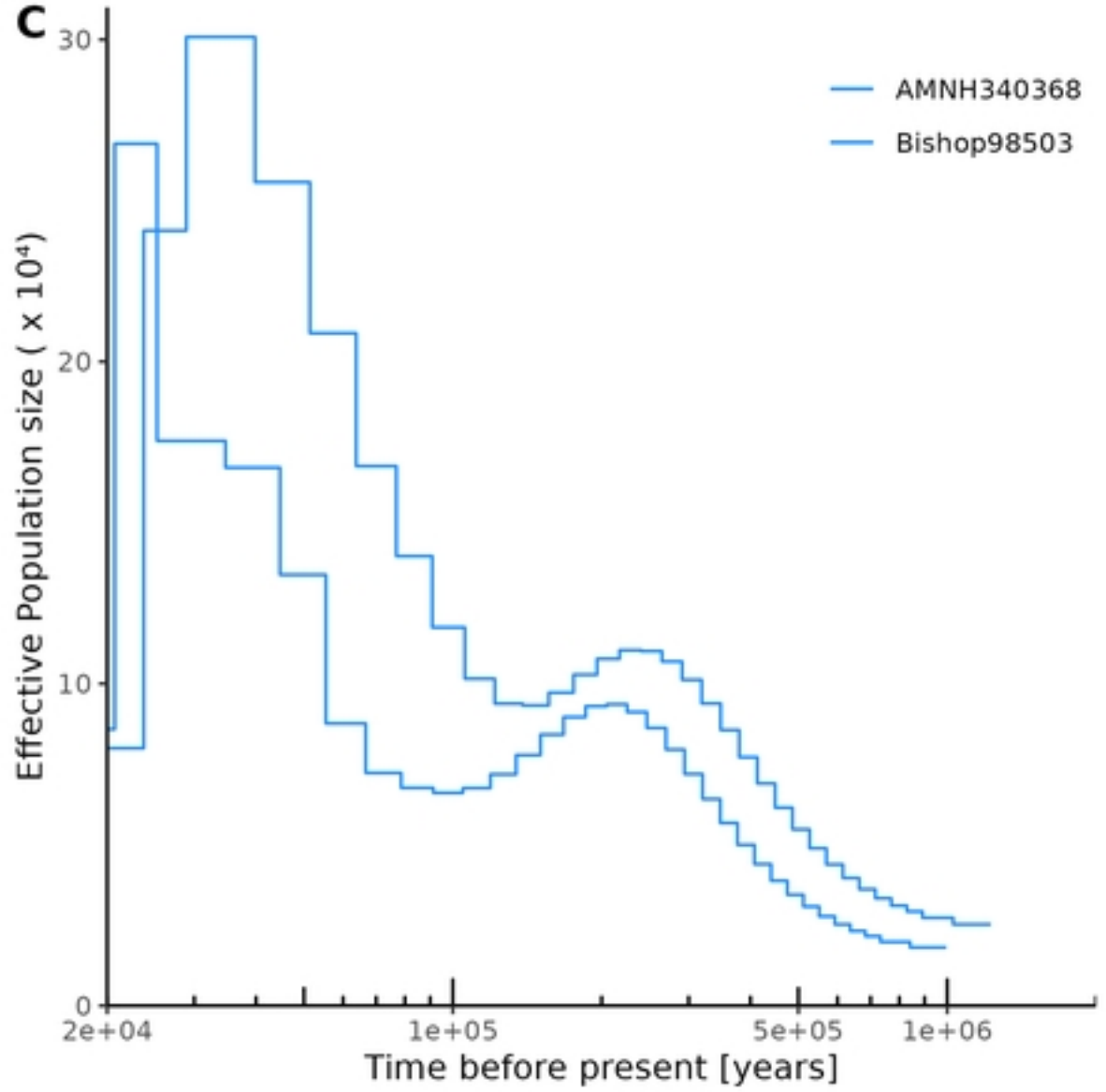

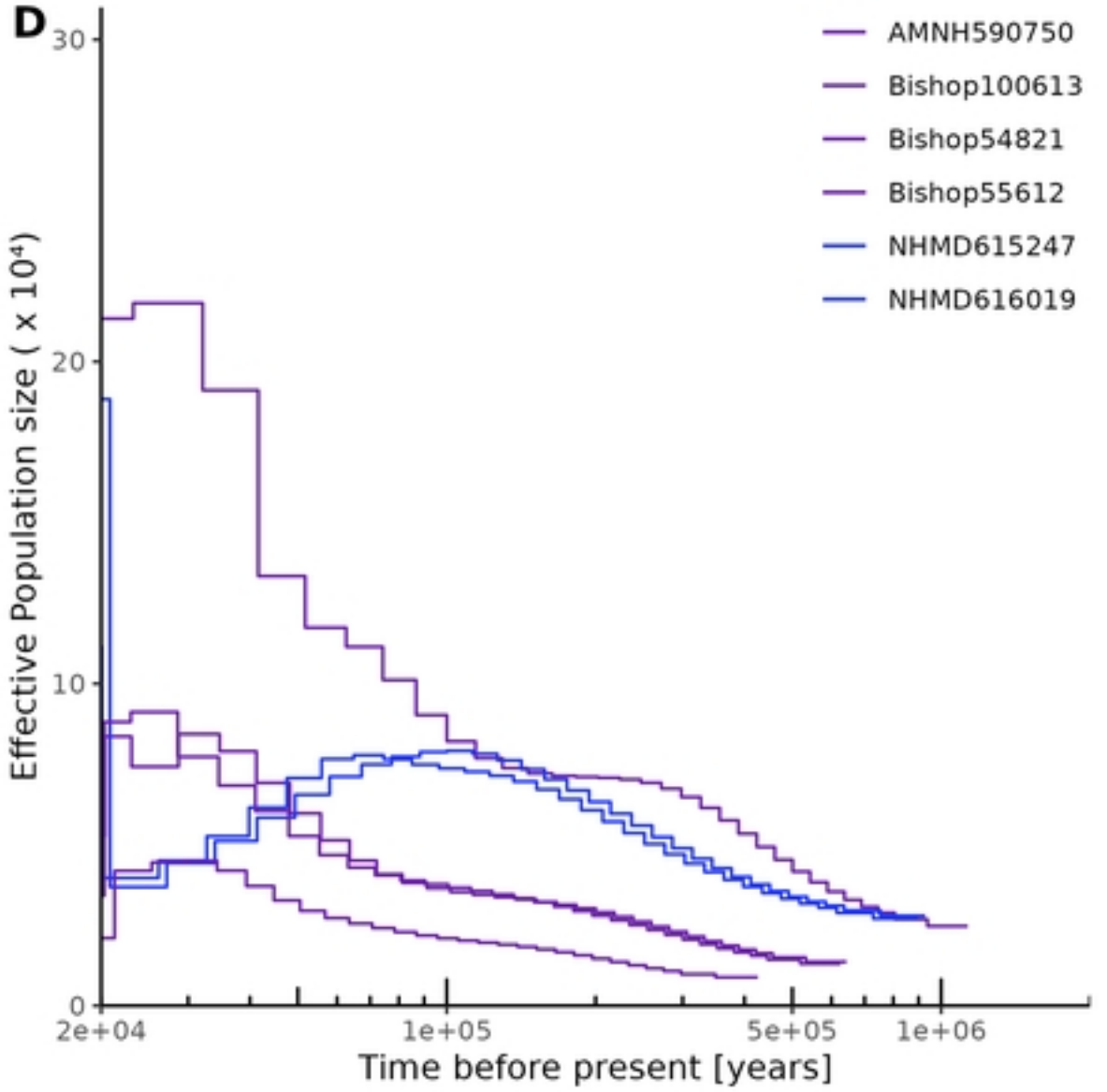

Main figure 3

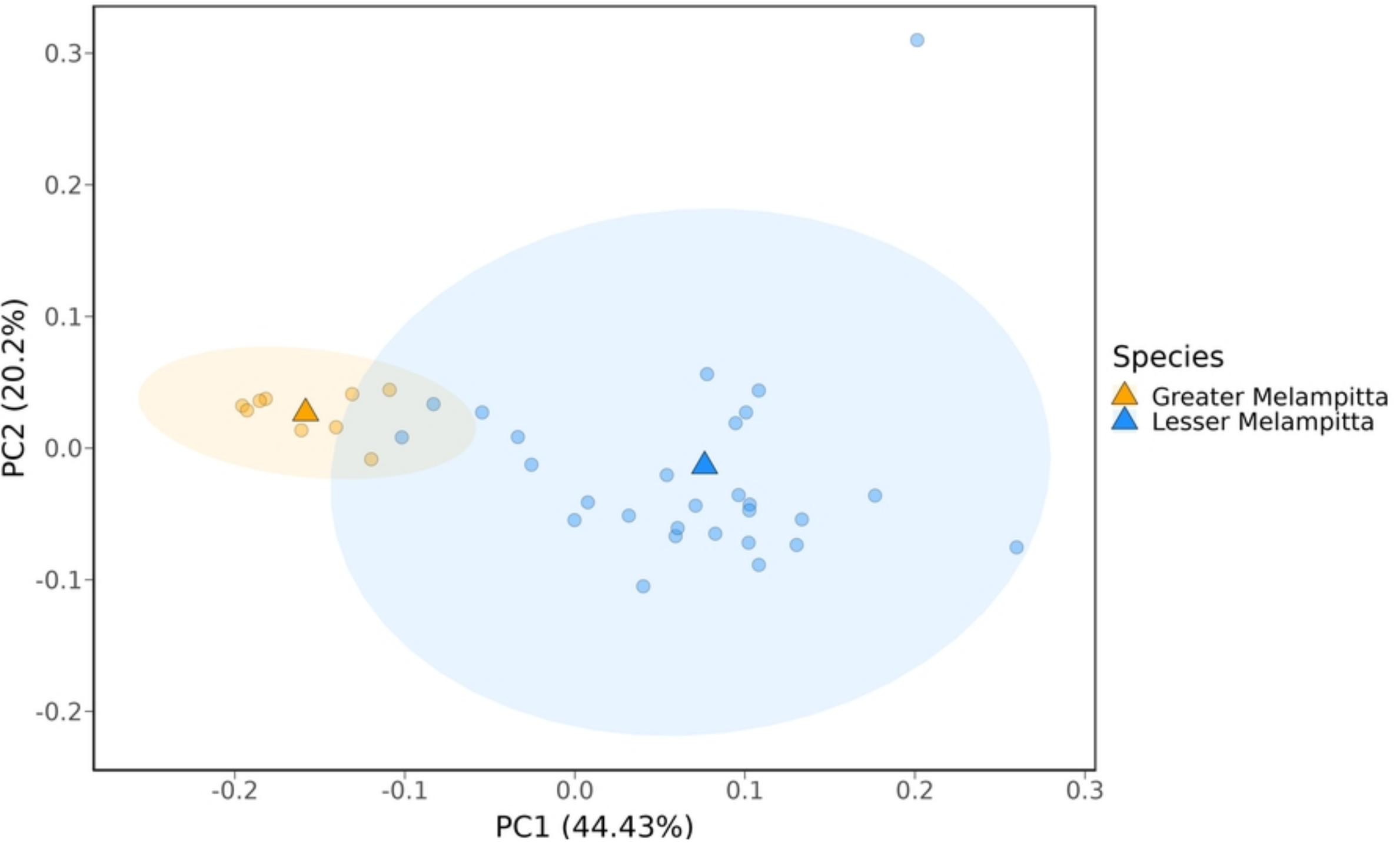

Main figure 4